# Simultaneous solitary-wave solutions in a nonlinear parametric waveguide

H. He, M. J. Werner, and P. D. Drummond
*Department of Physics, University of Queensland, St. Lucia, 4072, Australia*
(Received 7 December 1995; revised manuscript received 28 March 1996)

We introduce a simple topological classification for the solitary-wave solutions of the coupled equations describing $\chi^{(2)}$ parametric waveguides. Both temporal and spatial cases are studied. Simultaneous solitary-wave solutions at two different frequencies, which we term ''simultons,'' are shown to exist using topological arguments. In each case, families of general one-parameter simultons are given numerically. Each family consists of both fundamental and higher-order simultons of a topological or nontopological nature. There are several possible ways to combine dispersions at different frequencies. Thus there are more possible ways of maintaining temporal simultons in $1+1$ space-time than for purely spatial simultons in two space dimensions. [S1063-651X(96)10107-0]

PACS number(s): 42.65.Tg, 42.65.Ky

## I. INTRODUCTION

Solitary-wave solutions to the basic coupled equations describing the $\chi^{(2)}$ nonlinearity for equal group velocities, but including dispersion or diffraction, have been studied by many authors [1–18]. These results have shown that the two coupled partial differential equations have a wide range of solitary-wave solutions. The published solutions can be cast into three categories. The first is that the dynamics of an optical field traveling through a $\chi^{(2)}$ medium can be described by a nonlinear Schrödinger equation when there is large phase mismatching [2,6,7]. The second is that there are a few special cases of analytic solutions, found under strict phase-matching conditions [4,5,7–10], which we term ''simultons.'' Finally, there are simulton solutions found numerically [11–18], which extend the analytic cases into additional parameter regimes. The purpose of this paper is to introduce a systematic topological classification of all possible solitary-wave solutions. We include all cases presently known to exist, and demonstrate the existence of solutions that were previously unknown.

The equations that result when stationary conditions are applied are not integrable. In fact, they are closely related to those of the Hénon-Heiles chaotic Hamiltonian [19], which clearly has no general analytic solution. Despite this general lack of integrability, the equations have at least one integrable subspace, in which well-behaved and integrable solutions emerge. These do not have all the classical soliton properties — in particular, they are not invariant under collisions [7]. Despite this, the solutions can have excellent numerical stability, as demonstrated by numerical experiments at relatively low intensities. Chaotic behavior is also possible at higher intensities.

There are a number of interesting and unique features of this system of equations. Most significantly, they describe a novel type of nonlinear device — the parametric waveguide. This type of waveguide is potentially able to support very large nonlinearities when compared to the usual nonlinear refractive index devices. The reason for this is very simple — the parametric nonlinearity involves an $E^2$ as opposed to an $E^3$ nonlinearity. For this reason, it is typically a much stronger effect relative to the usual nonlinear refractive index, at low field intensities. Thus, we can anticipate a number of new types of solitonlike interactions being experimentally available at much lower field intensities than previously. Such strong nonlinearity has already been observed experimentally in self-phase modulation by DeSalvo *et al.* [20] and self-diffraction by Danielius *et al.* [21]. Nitti *et al.* [22] have obtained an increase of several orders of magnitude of the effective $\chi^{(3)}$ with an organic crystal of 2-($\alpha$-methylbenzylamino)-5-nitropiridine (MBA-NP).

These experimental results have stimulated more theoretical work on possible general simulton solutions. Solutions have been proven to exist numerically without satisfying strict phase-matching conditions [11–18]. However, although these general numerical solutions have greatly improved our understanding of this nonlinear system, the questions of whether all these solutions are complete, and how to classify them still remains unanswered. We are particularly interested here in temporal $(1+1)$-dimensional simultons, which can occur under a variety of conditions that are not possible for spatial cases. This question of general classification is especially important in view of the large number of solutions that are presently known.

One method of obtaining analytic solutions involves substituting an ansatz into the basic equations. It is impossible that all solutions can be found by using this method, due to the lack of integrability of the basic equations. Numerical solutions were also found by shooting methods, with the boundary conditions determined by preassuming the form of a solution. A complete and systematic way of finding simulton solutions is clearly needed, since the technique should not involve *a priori* assumptions.

In order to understand and classify the possible solitonlike or stationary-wave solutions, we introduce a topological classification. This allows an analysis of the equations without knowing the exact analytic solution — which is essential in view of the lack of integrability. Nevertheless, the topological technique can rule out those parameter values which are clearly *unable* to support solitary waves. Next, a numerical integration of the steady-state equation provides us with topologically acceptable candidate simultons, which exist for ranges of parameter values where no currently known analytic solutions occur. Finally, we determine the stability of the solution using a numerical solution of the complete partial differential equation, starting with a perturbed input,

 

close to the candidate simulton. The numerical analysis of the stability of these simultons is complex and lengthy, and will therefore be treated in a subsequent paper.

This topological method has proven to be very effective for both finding simulton solutions and providing explanations for the origins of these solutions. In this paper, we simplify the basic coupled equations to eight one-parameter equations. A simple mechanical analog can be applied to these equations. Using this analog, we can show by topological arguments that four cases do not have solitary-wave solutions. Using the topological method, all known solutions can then be classified into categories. In addition to these known solutions, we can also find other dark, bright, and hybrid type solitary-wave solutions for arbitrary phase-matching conditions. These solutions generally extend the known solutions into different regimes of dispersion and phase matching, thus relaxing the requirements for obtaining them experimentally.

We also demonstrate this topological method for finding two- and three-dimensional spatial simulton solutions. In addition to these previously known fundamental solutions [23,24,17], other general higher-order simultons representing the excited state of the fundamental solutions have also been found by this method.

Multiple-frequency solitary waves are found in resonant atomic interactions as well. This was originally suggested by Konopnicki *et al.* [25–27], Drummond [28], and, more recently, Grobe *et al.* [29] and Eberly *et al.* [30]. These solutions in a sense complement the parametric solitary waves treated here. The difference is that the cases studied here never involve resonant atomic excitation, and therefore have very low losses and fast response time, as is usual in nonlinear optical systems of this type.

In summary, the case of parametric simultons is interesting due to the relatively low losses and the possible technological applications inherent in these compact solid-state devices, as well as in the rich variety of new solutions.

## II. SIMPLIFICATION OF THE BASIC COUPLED EQUATIONS

We wish to treat the case of a time-dependent wave propagating in a one-dimensional, dispersive, parametric waveguide. The same equations, with some restrictions to the parameters, also can be used to treat a continuous wave (cw), propagating in a two-dimensional waveguide, or a three-dimensional medium with a transverse translational symmetry.

Based on the published model [5], we write the one-dimensional basic equation describing the cascaded $\chi^{(2)}$ parametric waveguide in the form

$$\left(\frac{\partial}{\partial z}+\frac{ik_1''}{2}\frac{\partial^2}{\partial t^2}\right)\phi_1=i\chi\phi_2\phi_1^*, \tag{1a}$$

$$\left(\frac{\partial}{\partial z}+\frac{ik_2''}{2}\frac{\partial^2}{\partial t^2}-i\beta\right)\phi_2=\frac{i\chi}{2}\phi_1^2, \tag{1b}$$

where $k_n''$ is the dispersion at the $n$th frequency, i.e., the derivative $d^2k/d\omega^2$ calculated at the point $k=k_n$. Here, $\beta=k_0^{(2)}-2k_0^{(1)}$ where $k_0^{(1)}$ and $k_0^{(2)}$ are wave numbers of the first and second harmonic, while the nonlinearity $\chi$ is given as

$$\chi=\frac{\epsilon_0\chi^{(2)}k_0^{(1)}}{\epsilon_1}\left(\frac{\hbar k_0^{(2)}}{2\epsilon_2}\right)^{1/2}\int d^2\mathbf{x}[u^{(1)}(\mathbf{x})]^2[u^{(2)}(\mathbf{x})]^*, \tag{2}$$

where $u^{(i)}(x)$ refers to normalized transverse-mode functions. The fields $\phi_1$ and $\phi_2$ are, respectively, the complex envelopes of the first and second harmonics, in units defined so that $|\phi_i|^2$ is the photon flux of the $i$th field. In this equation, it is assumed that the group velocities $v_i=d\omega/dk$ of the two fields match at the carrier frequency, to optimize simulton formation. For the convenience of comparison with other solitary-wave systems, we introduce characteristic scales of distance $z_0$ and time $t_0$ as well as photon number $p_i$ [31,32]:

$$z=z_0\xi, \tag{3a}$$

$$t=t_0\tau, \tag{3b}$$

$$p_1=|k_1''k_2''/(4t_0^3\chi^2)|, \tag{3c}$$

$$p_2=|(k_1'')^2/(4t_0^3\chi^2)|, \tag{3d}$$

where $t_0=\sqrt{|k_1''z_0|/2}$. The value of $t_0$ can be estimated from the ratio of a given pulse duration to that of the normalized simulton solution. Together with the dispersions and $\chi^{(2)}$ of the experimental material, values of $z_0$ and $p_i$ then can be determined. We will give an example in a subsequent section.

Using the variable transformation

$$\phi_1=|q|\sqrt{\left|\frac{k_2''}{k_1''}\right|}V_1e^{iqz}/\chi, \tag{4a}$$

$$\phi_2=-\mathrm{sgn}(k_1'')|q|V_2e^{i2qz}/\chi, \tag{4b}$$

we obtain the following dimensionless equations:

$$is_2\frac{\partial V_1}{\partial\xi}+\frac{\partial^2V_1}{\partial\tau^2}+V_1^*V_2-s_2V_1=0, \tag{5a}$$

$$is_2\sigma\frac{\partial V_2}{\partial\xi}+s_1\frac{\partial^2V_2}{\partial\tau^2}+\tfrac{1}{2}V_1^2-s_3\rho V_2=0, \tag{5b}$$

where

$$\xi=qz, \tag{6a}$$

$$s_1=\mathrm{sgn}(k_1''k_2''), \tag{6b}$$

$$s_2=-\mathrm{sgn}(k_1''q), \tag{6c}$$

$$s_3=-\mathrm{sgn}[k_1''(2q-\beta)], \tag{6d}$$

$$\sigma=|k_1''/k_2''|, \tag{6e}$$

$$\rho=|\sigma(2q-\beta)/q|. \tag{6f}$$

Here we let $|q|=z_0$, so there are two possible forms of scaled equations to consider for every distance scale. These correspond to inputs with nonlinear phase shifts of opposite signs. Physically, this is due to the fact that a $\chi^{(2)}$ medium is not inversion symmetric. It is sensitive to the relative phase of the two input fields. Different relative phases will give rise to different phase shifts, generating distinct possible types of soliton. For this reason, the scaled equation used here includes a scale parameter $q$ with arbitrary sign. Otherwise, $|q|=1/z_0$ is simply the inverse distance scale parameter.

The most general solutions written in polar variable form can be represented as

$$V_i=v_i(\xi,\tau)e^{i\theta_i(\xi,\tau)},\quad i=1,2, \tag{7}$$

where $v_i$ and $\theta_i$ are real.

Substituting these trial solutions into the above equations and using the stationary condition, for waves whose envelope function does not change under propagation,

$$\frac{\partial v_i}{\partial\xi}=0,\quad i=1,2, \tag{8}$$

we have

$$\frac{1}{v_1}\frac{\partial}{\partial\tau}\left(v_1^2\frac{\partial\theta}{\partial\tau}\right)+v_1v_2\sin(\theta_2-2\theta_1)=0, \tag{9a}$$

$$\frac{\partial^2 v_1}{\partial\tau^2}+v_1v_2\cos(\theta_2-2\theta_1)-v_1\left(\frac{\partial\theta_1}{\partial\tau}\right)^2-s_2v_1\left(\frac{\partial\theta_1}{\partial\xi}+1\right)=0, \tag{9b}$$

$$\frac{s_1}{v_2}\frac{\partial}{\partial\tau}\left(v_2^2\frac{\partial\theta_2}{\partial\tau}\right)+\tfrac{1}{2}v_1^2\sin(2\theta_1-\theta_2)=0, \tag{9c}$$

$$s_1\frac{\partial^2 v_2}{\partial\tau^2}+\tfrac{1}{2}v_1^2\cos(2\theta_1-\theta_2)-s_1v_2\left(\frac{\partial\theta_2}{\partial\tau}\right)^2-v_2\left(s_2\sigma\frac{\partial\theta_2}{\partial\xi}+s_3\rho\right)=0. \tag{9d}$$

These equations can be greatly simplified if we assume $\theta_1=K_1\xi$ and $\theta_2=K_2\xi$, where $K_1$ and $K_2$ are constant. This additional constraint means that we must now exclude the possibility of spatially chirped solutions, whose phase dependence is not just a linear function of $\xi$. If these did provide new solutions, they would form a new class of simultons.

Hence, Eqs. (9a) and (9c) become

$$\sin(\theta_2-2\theta_1)=0, \tag{10}$$

which gives $\theta_2=2\theta_1\pm n\pi, n\in N$.

The above result has a very important physical meaning, that the average wave number of the second harmonic must be twice the average wave number of the first harmonic in order to get stationary solutions. It also shows that changing the phase with the restriction $\theta_i=K_i\xi$, $i=1,2$, will not change the form of the equation, except for the value of $q$. Without losing generality, we therefore take $\theta_i=0$ for simplicity. We note that $q$, as introduced here, is effectively a nonlinear phase shift of the solution. Its value is determined implicitly by the initial conditions of the wave equation, and obviously depends on the intensity and duration of the input envelope function.

Equations (9b) and (9d) now become

$$\frac{\partial^2 v_1}{\partial\tau^2}+v_1v_2-s_2v_1=0, \tag{11a}$$

$$s_1\frac{\partial^2 v_2}{\partial\tau^2}+\tfrac{1}{2}v_1^2-s_3\rho v_2=0. \tag{11b}$$

The above equations significantly simplify the analysis for simulton solutions, since $v_i$ are real. Since each of $s_1, s_2$, and $s_3$ can have either sign, there are eight distinct cases to be examined.

## III. SIMULTON SOLUTIONS

The system given by Eq. (11) has a simple mechanical analog. The above equations can be read as the equations of motion of a virtual particle with unit mass in a potential, although the sign of the mass can change, depending on the coordinate. The trajectory of the virtual particle then corresponds to a pair of stationary solutions. Such mechanical analogies to static solutions have been pointed out by many people [33–36]. The new feature of the present equations is the possible anisotropy of the mass, which leads to new types of solution. The Hamiltonian of this system can therefore be written as

$$H=\tfrac{1}{2}p_1^2+\frac{s_1}{2}p_2^2+\tfrac{1}{2}v_1^2v_2-\frac{s_2}{2}v_1^2-\frac{s_3}{2}\rho v_2^2, \tag{12}$$

where $p_1=\dot{v}_1$ and $p_2=s_1\dot{v}_2$.

The potential is given as

$$V=\tfrac{1}{2}v_1^2v_2-\frac{s_2}{2}v_1^2-\frac{s_3}{2}\rho v_2^2. \tag{13}$$

However, this is not a normal Hamiltonian system because the particle may have a negative kinetic energy in the $v_2$ direction if $s_1<0$. We are only interested here in solutions which behave as isolated solitary waves, leaving the question of stability for later determination. We call such solutions simultons. Hence the following boundary conditions must be satisfied:

$$\frac{d^{(n)}v_1}{d\tau}=0,\quad \frac{d^{(n)}v_2}{d\tau}=0,\quad \tau=\mp\infty,\quad n=1,2,\ldots. \tag{14}$$

Thus the particle must stay at one of the points at which the above condition is satisfied. These points are called critical points. If a critical point is a simulton boundary, it must be unstable, otherwise a perturbation will produce periodic solutions. There are two types of simulton solutions, topological and nontopological, which start and end at nonoscillating critical points. Topological solutions have different boundary conditions for $\tau=\pm\infty$. Hence a potential possessing topological solutions must have at least two critical

points. Such a solution corresponds to a trajectory of the particle that connects two critical points. We call such a path a type-1 path.

Nontopological solutions have the same boundary conditions for $\tau=\pm\infty$, so the particle must be able to return to the starting critical point. Hence the path of the particle forms a loop. We call this path a type-2 path. The path may be a reversible curve that connects the critical point and a point in the potential at which $dv_i/d\tau=0$, $i=1,2$, but $d^{(n)}v_i/d\tau^n \neq 0$, $n=2,3,\ldots$, $i=1,2$. Such a path is a special case of a type-2 path. We call it a type-3 path.

At any one of these critical points, the gradient of the potential must be zero. Hence, critical points must satisfy

$$v_1 v_2 - s_2 v_1 = 0, \tag{15a}$$

$$\tfrac{1}{2} v_1^2 - s_3 \rho v_2 = 0. \tag{15b}$$

Three critical points are found at (0,0) and $(\pm\sqrt{2 s_2 s_3 \rho}, s_2)$. Note that only one critical point exists at (0,0) when $s_2 s_3 < 0$. We have studied cases with $s_2 s_3 < 0$ and found no possible type-2 or type-3 paths, which eliminates the possibility of simulton solutions. Thus simulton solutions can only occur if $s_2 = s_3$. We therefore have decreased the number of different cases from eight to four.

The system described by Eq. (11) is a Hamiltonian system. Hence the total energy is conserved. A particle that starts from (0,0) has energy of $H=0$. A particle that starts from $(\pm\sqrt{2\rho}, s_2)$ has an energy of $H=-s_2 \frac{1}{2}\rho$. Since the energy at (0,0) is different from those of the other two (unless $\rho=0$), it is impossible for a particle starting from (0,0) to reach one of the other points with its speed approaching zero, or vice versa.

The remaining task is to find all possible simulton paths. The motion of the virtual particle can be very complex in the potential. A novel feature of this problem is the existence of paths for a particle whose mass has different signs in different coordinates. An effective approach to overcome this problem is to consider Eq. (11) as Newtonian acceleration equations with acceleration field given by

$$\vec{F} = [s_2 v_1 - v_1 v_2, s_1 s_2 \rho v_2 - s_1 \tfrac{1}{2} v_1^2]. \tag{16}$$

There are four different acceleration fields corresponding to different signs of $s_1$ and $s_2$, with $s_2 s_3 > 0$. We define a ''case vector,'' case$(s_1, s_2)$, for convenience of discussion.

There are many advantages of drawing acceleration fields. Most importantly, it allows a classification of all critical points without actually solving the equation. It can also give qualitative predictions about the form of simulton solutions and their existence over a range of parameters. We now proceed to show more details.

Linearized around a critical point, the above Newtonian system can be written in the form

$$\dot{\vec{v}} = \mathbf{A}\vec{v}, \tag{17}$$

where $\mathbf{A}$ is a real $2\times 2$ matrix.

Obviously, the solutions to Eq. (17) can be written in the form $\vec{v} = \Sigma_{n=1,2} \vec{c}_n e^{\beta_n \tau}$. We find $\beta_n = \pm\sqrt{\lambda_{1,2}}$ where $\lambda_{1,2}$ are the eigenvalues of $\mathbf{A}$. Since $\mathbf{A}$ is a $2\times 2$ matrix, $\lambda_{1,2}$ are just solutions of a quadratic with $\lambda_1 + \lambda_2$ real. Hence the cases are

$$\lambda_{1,2} < 0, \tag{18a}$$

$$\lambda_1 > 0, \quad \lambda_2 < 0, \tag{18b}$$

$$\lambda_{1,2} > 0, \tag{18c}$$

$$\lambda_{1,2} = a \pm ib, \tag{18d}$$

corresponding to four different cases of $\beta$ being of the form

$$\pm ix, \quad \pm iy, \tag{19a}$$

$$\pm x, \quad \pm iy, \tag{19b}$$

$$\pm x, \quad \pm y, \tag{19c}$$

$$x \pm iy, \quad -x \pm iy. \tag{19d}$$

Due to the relationship between the values of $\lambda$ and the values of $\beta$, we can classify the end points of solutions of the Newtonian equation simply from the form of its acceleration field. The first case, describing a stable point, only leads to stable periodic solutions with no corresponding simulton solutions. All the other cases lead to unstable critical points, which can therefore correspond to simultons. When we have an unstable critical point with accelerations pointing outward, its solutions are always unstable. If we have a saddle point in the acceleration field, then the solution can only be unstable or periodic. If an acceleration field has a spiral structure, then the solution also takes similar spiral forms with an infinite number of unstable paths. The eigenvalues of $\mathbf{A}$ can be easily found:

$$\lambda_1 = s_2, \quad \lambda_2 = s_1 s_2 \rho \tag{20}$$

for an equation linearized around point (0,0) and

$$\lambda_{1,2} = (s_1 s_2 \rho \pm \sqrt{\rho^2 + 8 s_1 \rho})/2 \tag{21}$$

for an equation linearized around $(\pm\sqrt{2\rho}, s_2)$.

When a particle on a simulton path approaches an ordinary critical point (a point with real eigenvalues), its speed approaches zero as $\tau \to \pm\infty$. In order to achieve this, the acceleration must have one component along the path of the particle. Therefore simulton solutions are possible only if the acceleration field has at least one acceleration line pointing outward. If the accelerations have constant direction near a critical point, then the trajectory of the particle, near the point, becomes a straight line and is the same as the acceleration lines near the point.

The behavior of a particle around a complex critical point (a point with complex eigenvalues) becomes very complicated and interesting. Even if a complex point has accelerations pointing in, it still has unstable paths. Since the whole process is always symmetric in the time domain, a particle can always follow these paths back with its speed also approaching zero. Thus any type of spiral field of acceleration vectors can lead to unstable paths.

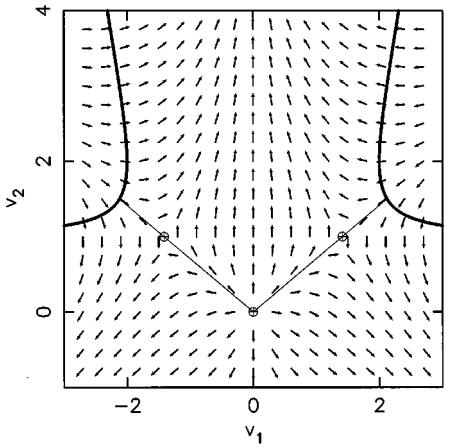


FIG. 1. Acceleration field for case$(+,+)$ at $\rho=1$, including the boundary (heavy line) at $E=0$, and a phase-space projection of its fundamental simulton solution (light line): $v_1=\pm[3/(2)^{1/2}]\,\mathrm{sech}^2(\tau/2)$, $v_2=(3/2)\mathrm{sech}^2(\tau/2)$.

An acceleration field can also provide information about the range of possible trajectories of a particle, since a particle is able to come back to its starting point only if it encounters an opposing acceleration. Therefore, without actually solving the original equations, the acceleration field can indicate the existence of simulton solutions, their forms, and the ranges of their parameters. Under these guidelines, numerical simulton solutions can then be found systematically, using standard numerical techniques.

Using the above techniques, we first consider the simplest case, $\rho=0$, with the acceleration field being of the form

$$\vec{F}=[(s_2v_1-v_1v_2),-s_1\tfrac{1}{2}v_1^2]. \tag{22}$$

The system does not have any simulton solutions, because the acceleration along $v_2$ $(-s_1\,\frac{1}{2}\,v_1^2)$, never changes its sign under any situation. Hence the particle will never be able to return to its starting point. Therefore, no simulton solutions are possible.

We next consider different cases separately according to the signs of $s_1$ and $s_2$.

### A. case(+,+)

#### *1. Fundamental simultons*

In this case, as shown in Fig. 1, the acceleration field has three critical points. Among them, the points $(\pm\sqrt{2\rho},1)$ are saddle points. The acceleration field in the unstable direction of the saddle points does not allow a return path to a critical point. Therefore no simulton solution is possible if a particle starts from one of these saddle points. Another critical point is at (0,0), with acceleration vectors pointing to all directions evenly. There are an infinite number of possible paths passing this point. In the upper left and upper right in Fig. 1, there are accelerations pointing to (0,0). The simplest possible case is that a particle starts from (0,0) and then goes to upper left or upper right and then returns, forming a nontopological simulton. The system has a normal Hamiltonian and it can be described by the following equations of motion:

$$\ddot{v}_1+v_1v_2-v_1=0, \tag{23a}$$

$$\ddot{v}_2+\tfrac{1}{2}v_1^2-\rho v_2=0. \tag{23b}$$

We find, at the starting point, that $H_{(0,0)}=0$. Hence, at all times,

$$H=\tfrac{1}{2}p_1^2+\tfrac{1}{2}p_2^2+\tfrac{1}{2}v_1^2v_2-\tfrac{1}{2}v_1^2-\tfrac{1}{2}\rho v_2^2=0. \tag{24}$$

The motion of a particle starting from (0,0) is therefore confined by the boundary given by

$$\tfrac{1}{2}v_1^2v_2-\tfrac{1}{2}v_1^2-\tfrac{1}{2}\rho v_2^2=0, \tag{25}$$

which gives

$$v_1=\pm\sqrt{\frac{\rho}{(v_2-1)}}v_2. \tag{26}$$

These two boundaries are shown as heavy curves in Fig. 1.

We now are able to prove the existence of nontopological or type-3 simultons, using the acceleration field with the aid of the above results. A type-3 path is symmetric with time, and the energy is conserved. A particle on this path must have coordinates satisfying the above equation, with velocity equal to zero at $\tau=0$. It then returns along the same path. All accelerations along the upper part of the boundary have components pointing upward while those along the lower part of the boundary have components pointing downward. If a particle is along the upper part of the boundary, it will pass over (0,0). If it is along the bottom part of the boundary, it will pass under (0,0). Since the boundary is continuous, there must be a point along the boundary from which a particle can approach (0,0) as $\tau\to\pm\infty$. Changing the value of $\rho$ only changes the position of the boundary, but will not change the topological structure of the acceleration field: the eigenvalues of **A** always take the same form for this case. In other words, we can always find positions along the boundary such that the path will pass over (0,0) or under (0,0). Therefore such solutions always exist for any nonzero value of $\rho$. Note that $\rho$ is always positive by definition.

In order to find the path, we assume $v_1=v_1(v_2)$. Hence,

$$\ddot{v}_1=v_1''(\dot{v}_2)^2+v_1'\ddot{v}_2, \tag{27}$$

where $v_1'=\partial v_1/\partial v_2$. Combining Eq. (24) with Eq. (23) we have

$$v_1(1-v_2)=v_1''\frac{v_1^2+\rho v_2^2-v_1^2v_2}{(v_1')^2+1}+v_1'(\rho v_2-\tfrac{1}{2}v_1^2). \tag{28}$$

The simplest path is a straight line. Inserting the form $v_1=rv_2$, where $r$ is a constant, into the above equation, we find that $r=\sqrt{2}$ providing

$$\rho=1. \tag{29}$$

Substituting these conditions into Eq. (23), we have

$$\ddot{v}_2+v_2^2-v_2=0, \tag{30}$$

which is integrable. The solutions to Eqs. (23) are given as

$$v_1 = \pm \frac{3\sqrt{2}}{2} \mathrm{sech}^2\left(\frac{\tau}{2}\right), \tag{31a}$$

$$v_2 = \frac{3}{2} \mathrm{sech}^2\left(\frac{\tau}{2}\right). \tag{31b}$$

This pair of solutions was found by Werner and Drummond [5] and others [1,8]. Note the condition $\rho = 1$ is equivalent to the phase-matching condition, as appeared in [5].

As we proved above, there is always a simulton solution regardless of the value of $\rho$. Since Eq. (28) is generally nonintegrable for arbitrary values of $\rho$, general analytic solutions are not easily available. However, based on the arguments given above about the acceleration field, it is trivial to obtain general solutions numerically. We simply choose a point along the boundary, Eq. (26), as the boundary condition and then integrate Eq. (23) numerically by trial and error. Solutions with errors below $10^{-10}$ can easily be obtained using this standard shooting technique.

We have obtained a whole range of numerical simulton solutions for many values of $\rho > 0$. Paths corresponding to different values of $\rho$ with values $\rho = 0.1$, 0.5, 1.0, 3.0, and 10.0 are shown in Fig. 2(a). These paths can be regarded as ''phase projections'' of the four-dimensional phase space of this system onto the two-dimensional $v_1$-$v_2$ plane. Simulton profiles are shown in Fig. 2(b) and Fig. 2(c). Similar results of these fundamental simulton solutions were reported by Buryak and Kivshar [11,18] and Torner *et al.* [13,14]. From Fig. 2(a), we can see that when $\rho = 1$ the path is a straight line which agrees with the analytical solution. We can think of these paths balancing between upward accelerations and downward accelerations. When $\rho > 1$, upward accelerations are generally higher than downward accelerations, so paths bend slightly upward to reach a balance. When $\rho < 1$, downward accelerations are bigger and paths therefore bend slightly downward.

To observe these temporal simultons experimentally, the following conditions must be satisfied: (1) a suitable waveguide with strong second order nonlinearity must be used; (2) the group velocities of the two harmonics must be matched; (3) most importantly, the material must be highly dispersive in order to verify the formation of simultons. The last condition is currently the most difficult one. Among the known optical materials, organic materials have been reported to be most dispersive [22]. Even if such a material is used, its dispersion ($\approx 1\,\mathrm{ps}^2/\mathrm{m}$) together with a 100 fs laser pulse only implies a dispersive scale length on the order of 1 cm [9]. As an example, we consider a waveguide made of $LiNbO_3$. We use the following values: $\chi^{(2)} = 11.9$ pm/V [37] and wavelength of the first harmonic $\lambda = 1.06$ $\mu$m. Suppose $\beta = 0$ and $\sigma = 1/2$, we then have $\rho = 1$. Assuming a dispersion $k_1''$ of $0.1\,\mathrm{ps}^2/\mathrm{m}$, a pulse width (defined as full width at $1/e$ intensity) of 100 fs, and a waveguide area of 100 $\mu\mathrm{m}^2$, we find that $\chi \approx 4 \times 10^{-8}\ \mathrm{s}^{1/2}\,\mathrm{m}^{-1}$. The characteristic scale values are $t_0 \approx 30$ fs, $z_0 \approx 2$ cm, $p_1 \approx 1 \times 10^5$ photons per pulse, and $p_2 \approx 5 \times 10^4$ photons per pulse. For a 1 GHz repetition rate, this corresponds to an average power of the order of $10^{-4}$–$10^{-5}$ W, with a peak power around 1 W. These figures demonstrate the low power levels possible in soliton formation with a $\chi^{(2)}$ waveguide, relative to a $\chi^{(3)}$ waveguide.

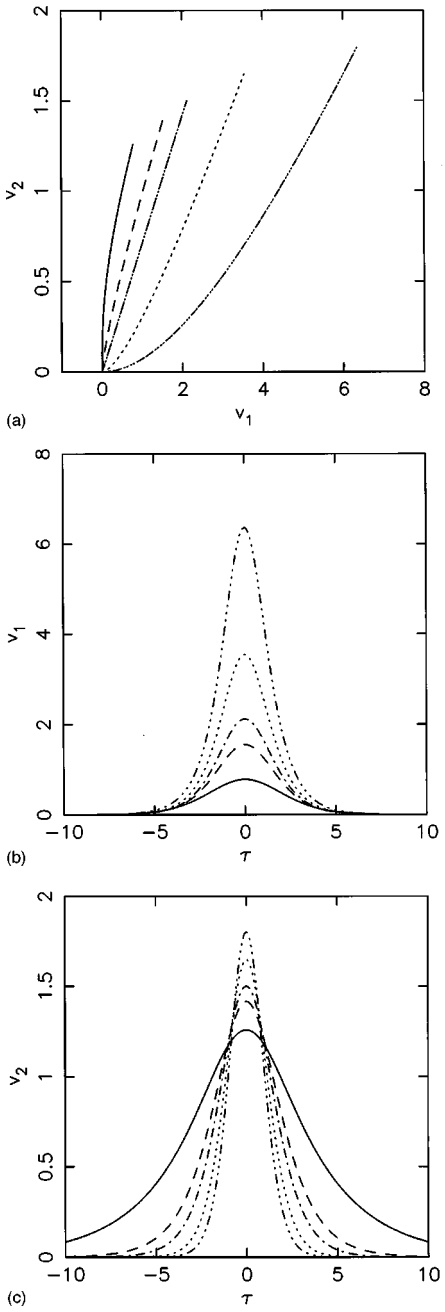


FIG. 2. Fundamental simulton solutions for case$(+,+)$. (a) Phase-space projections where $\rho = 0.1$ (solid line), 0.5 (dashed line), 1.0 (dash-dot line), 3.0 (dotted line), and 10.0 (dash-dash-dot-dot line); (b) simulton time evolution of $v_1$; (c) simulton time evolution of $v_2$.

#### *2. Higher-order simultons*

A virtual particle can also be reflected from one side of the boundary and reach the other side. It can then either approach the point (0,0) or be reflected again. This process can repeat as many times as possible, which introduces a whole family of higher-order simulton solutions. We identify each higher-order simulton solution of this type as

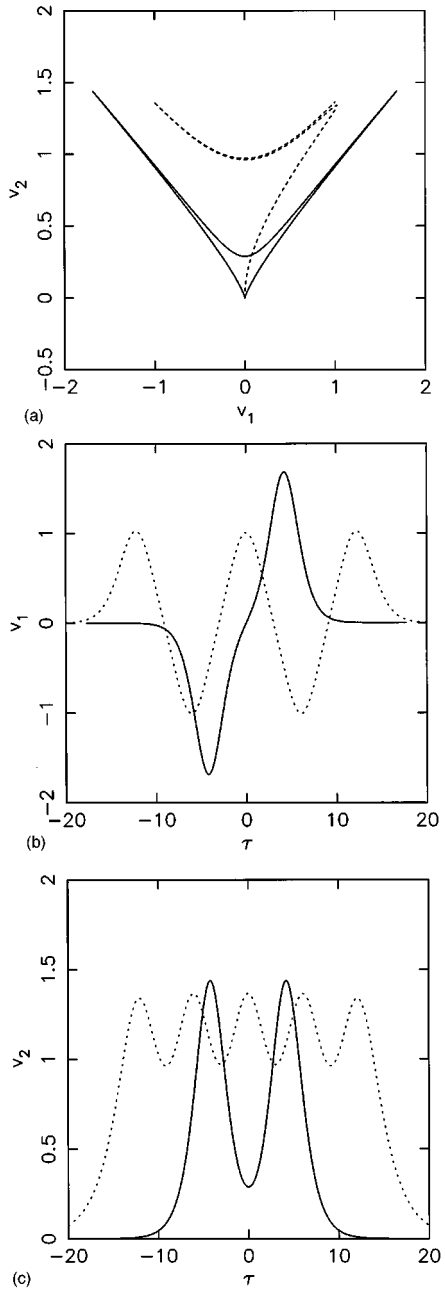


FIG. 3. Higher-order simulton solutions for case(+,+). In order to avoid overlap, we choose different values of $\rho$ for different orders: the solution $n=2$ has $\rho=0.6$ (solid line) and the solution $n=5$ has $\rho=0.2$ (dotted line). (a) Phase-space projections; (b) simulton time evolution of $v_1$; (c) simulton time evolution of $v_2$.

$v_i^n$, $i=1,2$, $n=0,1,2,\ldots,\infty$, where $n$ is how many times the virtual particle is reflected from the boundaries after it starts from the point (0,0). When $n\to\infty$, we then have a pair of nonlinear periodic solutions. Clearly, $n=1$ gives the ordinary one-peak simulton solutions. Such a multipeak simulton has $n$ peaks.

To show the above bouncing process, paths of $\rho=0.6$ with two peaks and $\rho=0.2$ with five peaks are shown as Fig. 3(a). Numerical solutions for $v_1$ and $v_2$ are shown in Fig. 3(b) and Fig. 3(c), respectively. The amplitudes of these solutions increase as $\rho$ increases.

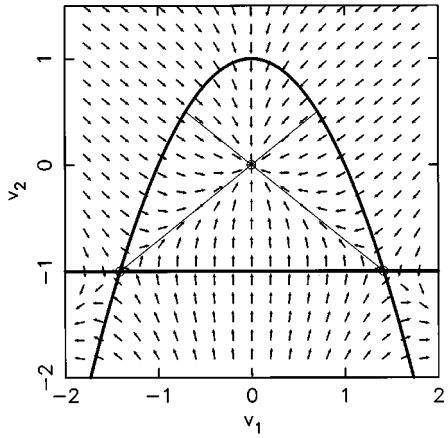

FIG. 4. Acceleration field for case(+,−) at $\rho=1$ including the boundary (heavy line) at $E=\rho/2$, and the phase-space projection of the solution (light line): $v_1=\pm(2)^{1/2}[(3/2)\ \mathrm{sech}^2(\tau/2)-1]$, $v_2=(3/2)\mathrm{sech}^2(\tau/2)-1$.

### B. case(+,−)

The system now takes the form

$$\ddot{v}_1+v_1v_2+v_1=0, \tag{32a}$$

$$\ddot{v}_2+\tfrac{1}{2}v_1^2+\rho v_2=0. \tag{32b}$$

The acceleration field of this system is shown as Fig. 4.

First, we note that its topological structure is independent of the value of $\rho$, as **A** never changes its form regardless of the value of $\rho$. The eigenvalues around point (0,0) are always negative and these around point $(\pm\sqrt{2\rho},-1)$ always have different signs. Point (0,0) is stable and hence no simulton solution is possible if a particle starts from this point. The other two critical points at $(\pm\sqrt{2\rho},-1)$ are saddle points.

Second, the system is a normal Hamiltonian system, as all ''masses'' are positive ($s_1>0$). The Hamiltonian of a particle that starts from either one of these two points is $\frac{1}{2}\rho$. As a result, the motion of the particle is confined in the area surrounded by

$$v_2=\frac{v_1^2-\rho}{\rho}, \tag{33a}$$

$$v_2=-1. \tag{33b}$$

The boundary which passes through the two saddle points is shown in Fig. 4 in heavy lines. Since these two points are saddle points as shown in Fig. 4, only two paths pass through each of them. One path is stable. The other is unstable, being of the form

$$v_2=\mp\sqrt{\frac{\rho}{2}}v_1 \tag{34}$$

near the saddle points.

After being perturbed toward the confined area, a virtual particle will keep its motion inside the area. The particle will stop only if it reaches the other saddle point or returns to the starting saddle point. Note that the unstable path passing each one of the saddle points is unique for every value of $\rho$. In some cases, when $\rho$ takes a particular value, the paths

of the virtual particle become simulton paths of both topological and nontopological nature. As a result, these paths form a family of discrete simulton solutions, as pointed out by Buryak and Kivshar [15].

The simplest form of these paths is a straight line. The unstable paths passing these two saddle points can be written as

$$v_2 = \mp \sqrt{\frac{\rho}{2}} v_1. \tag{35}$$

Now the path equation becomes

$$-v_1(1+v_2) = v_1'' \frac{-v_1^2 - \rho v_2^2 - v_1^2 v_2}{(v_1')^2 + 1} - v_1'(\rho v_2 + \tfrac{1}{2} v_1^2). \tag{36}$$

Substituting $v_1 = \sqrt{2/\rho} v_2$ into the above equation we find $\rho = 1$. This is a straight line that passes (0,0) and $(\sqrt{2}, -1)$. Equation (32b) becomes

$$\ddot{v}_2 + v_2^2 + v_2 = 0. \tag{37}$$

Shifting to $(-\sqrt{2}, -1)$, we have $V = v_2 + 1$, so the above equation becomes

$$\ddot{V} + V^2 - V = 0. \tag{38}$$

We have solved this equation in the previous case and the solution is

$$V = \frac{3}{2} \mathrm{sech}^2\left(\frac{\tau}{2}\right). \tag{39}$$

Hence, we have solutions

$$v_1 = \pm \sqrt{2}\left[\frac{3}{2} \mathrm{sech}^2\left(\frac{\tau}{2}\right) - 1\right], \tag{40a}$$

$$v_2 = \frac{3}{2} \mathrm{sech}^2\left(\frac{\tau}{2}\right) - 1. \tag{40b}$$

The above solutions were found previously [9,8,10] as a novel type of dark simultons. However, because the particle starts from either one of these two saddle points, the corresponding simulton solutions appear with a bright cw background, $v_1 = \pm\sqrt{2}, v_2 = 1$. However, the continuous wave (cw) background is not stable due to modulational instability, as both the dispersions take the same sign [38,39,15]. Thus, although there exists a family of discrete simulton solutions, they are all unstable due to the same modulational instability. We therefore do not analyze this case further.

### C. case(−,+)

One of the important features of this system is that $s_1 = -1$ — with one direction of the mass tensor effectively negative, the system is no longer a normal Hamiltonian system. Compared with the previous two cases, the motion of a virtual particle is no longer confined by boundaries. This has obviously increased the variety of simultons of this case, as there are more possibilities of forming different simulton paths.

The acceleration field shown in Fig. 5 reveals three unstable critical points. Since they have distinct values of the Hamiltonian, we then have two categories of simulton solutions: (1) simultons associated with the saddle point (0,0) and (2) simultons associated with the other two points at $(\pm\sqrt{2\rho}, 1)$.

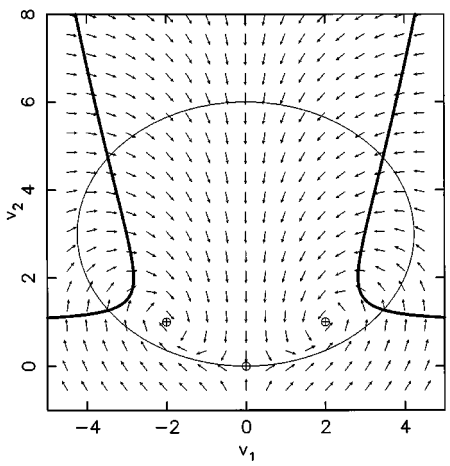


FIG. 5. Acceleration field for case(−,+) at $\rho = 2$ including the boundary (heavy line) at $E = 0$, and the phase-space projection of the solution (light line): $v_1 = 6(2)^{1/2}\mathrm{sech}(\tau)\tanh(\tau)$, $v_2 = 6\mathrm{sech}^2(\tau)$.

#### *1. Simultons associated with point (0,0)*

The critical point (0,0) is a saddle point for any value of $\rho$, as the eigenvalues around it always take different signs. It only has one unstable path along the $v_2 = 0$ axis near (0,0) for each value of $\rho$, as shown in the acceleration field. It is obvious that only nontopological simulton solutions (type 2 and type 3) are possible. Since the path is unique to each value of $\rho$, the path depends solely upon the value of $\rho$. Varying the value of $\rho$ gives a whole range of paths.

After leaving (0,0), a particle will go upward due to the upward accelerations along the $v_2 = 0$ axis. Its direction of motion will be bent toward the axis $v_1 = 0$ because of accelerations pointing toward $v_1 = 0$. Its path will be bent further due to downward accelerations near the vertical axis. There are three possibilities when the particle crosses the axis $v_1 = 0$: (1) $p_2 = 0$; (2) $p_2 < 0$; (3) $p_2 > 0$. The first possibility indicates a type-2 path, as the acceleration field is always symmetric with the axis $v_1 = 0$. In the second situation, the path of the particle will follow the spiral structure of the acceleration field. This does not allow a return or closed path. Hence no simulton is possible. In the last case, the particle will encounter opposite accelerations when it is moving upward — a type-3 path is possible. If the particle does not meet the requirement of forming a type-3 path, it can still cross the axis $v_1 = 0$ again with the same three possibilities as it met before. The process is then repeated and can be repeated for as many times as possible. The existence of these simulton solutions can therefore be proved, as the change of the orientation of the path is continuous when $\rho$ changes. The above process also suggests that these simultons can be classified by the number of peaks of $v_1$, i.e., $v_i^{(n)}, n = 2,3, \ldots$. For example, a simulton of this category with two peaks can be identified as $v_i^{(2)}$.

Based on the above knowledge of this case, each simulton can be solved numerically by using a modified shooting

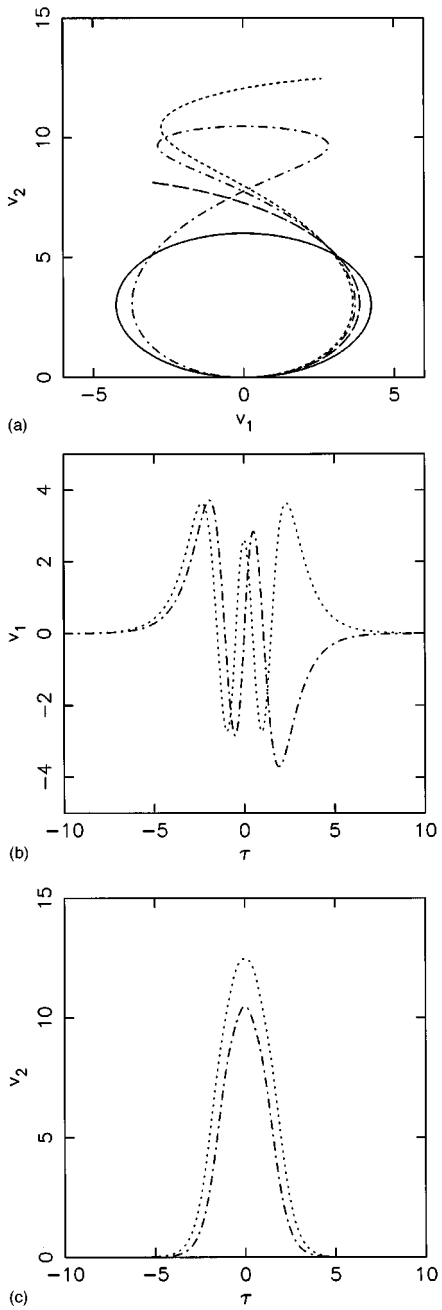


FIG. 6. Simultons associated with (0,0) for case$(-,+)$. (a) Phase-space projections of $v_i^{(2)}$ (solid line), $v_i^{(3)}$ (dashed line), $v_i^{(4)}$ (dash-dotted line), and $v_i^{(5)}$ (dotted line); (b) simulton time evolutions of $v_1^{(4)}$ (dash-dotted line) and $v_1^{(5)}$ (dotted line); (c) simulton time evolutions of $v_2^{(4)}$ (dash-dotted line) and $v_2^{(5)}$ (dotted line).

method. When $\rho=2$, there is a type-2 path, a $v_i^{(2)}$ solution. This solution, first found analytically by Werner and Drummond [5], takes the form

$$v_1=\pm 6\sqrt{2}\,\mathrm{sech}(\tau)\tanh(\tau), \tag{41a}$$

$$v_2=6\,\mathrm{sech}^2(\tau). \tag{41b}$$

Solution $v_i^{(3)}$ is obtained when $\rho\approx 1.03$. Other simultons with more peaks are found at smaller values of $\rho$.

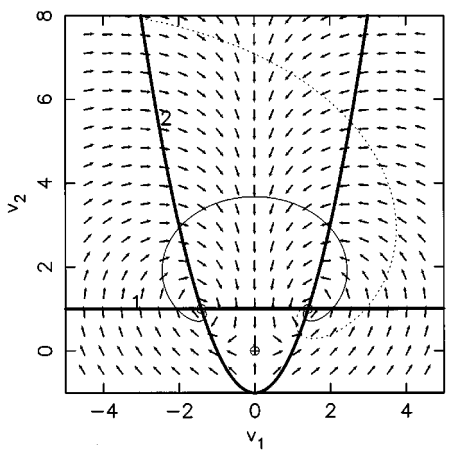


FIG. 7. Acceleration field for case$(-,+)$ at $\rho=1$ including the boundary (heavy line) at $E=-\rho/2$ (the boundary $v_2=v_1^2/\rho-1$ is labeled with 2 and the boundary $v_2=1$ is labeled with 1), and the phase-space projection of a fundamental type-1 simulton solution (light solid line) and a fundamental type-3 simulton solution (light dotted line).

Numerically generated paths of these simultons at $n=2,3,4,$ and 5 are shown in Fig. 6(a). Some typical simulton profiles are shown in Fig. 6(a) and Fig. 6(b).

#### *2. Simultons associated with points $(\pm(2\rho)^{1/2},1)$*

Simultons associated with points $(\pm\sqrt{2\rho},1)$ will appear with a bright cw background because of the nonzero values of these two points. Therefore these solutions must satisfy the modulational stability conditions published in our previous paper [38]. One of the necessary stability conditions is $\rho\leqslant 2$ for this case. Within such a range, the eigenvalues around these two points always take complex values, and hence the topological structure of the acceleration field is invariant for $\rho\leqslant 2$. Although all accelerations point toward these two points, they are unstable critical points. As we proved previously, unstable paths exist with spiral structures even for inward-spiraling acceleration fields. The actual simultons hence would appear with oscillating tails. From the acceleration field, we can see that both type-1 and type-3 paths are possible. Type-2 paths may be possible. However, no type-2 paths were found during numerical scanning within possible ranges. Again, due to the symmetry of the acceleration field, higher-order type-1 and type-3 paths exist. Similar approaches to the previous cases are adopted for finding these simultons. A type-1 path connecting these two spiral points is symmetric about the vertical axis $v_1=0$. Therefore there must be a point along the axis at which $\dot{v}_2=0$. The position of the point can be then found numerically by trial and error. Since there are an infinite number of paths connecting these two points, we can always find such simulton solutions for any value of $\rho<2$. Note that the particle can cross the axis $v_1=0$ as many times as possible; points with $\dot{v}_2=0$ can also be found at higher values of $v_2$, which correspond to different higher-order simulton solutions. Using the shooting technique, we then can generate a whole family of higher-order type-1 simultons.

A type-3 path always has a turning point at which $\dot{v}_i=0$. Such a point must be along the boundary

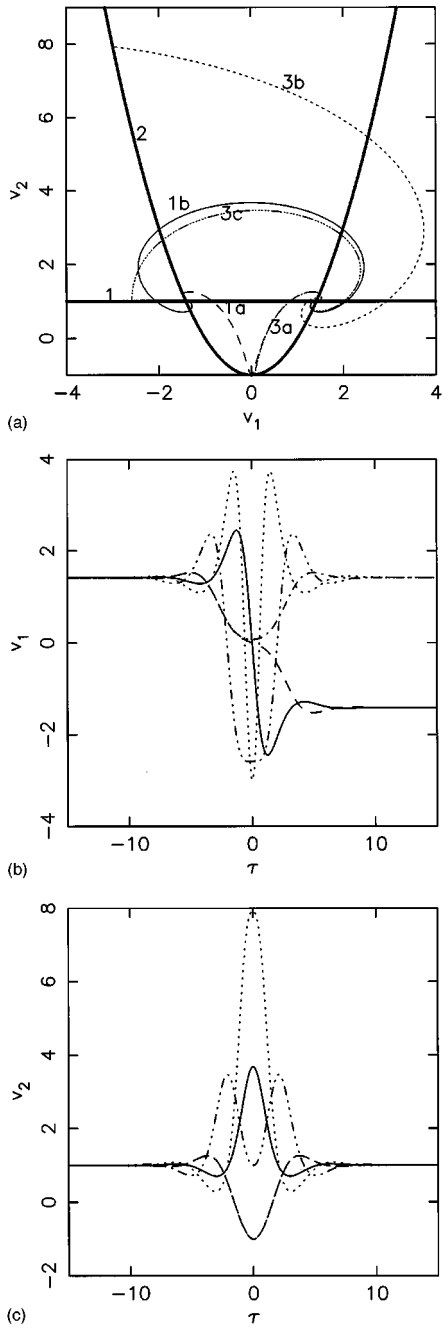


FIG. 8. Fundamental simultons associated with $(\pm(2\rho)^{1/2},1)$ for case$(-,+)$ at $\rho=1$. Solution 1a (dashed line); solution 1b (solid line); solution 3a (dash-dot line); solution 3b (dotted line); solution 3c (dash-dot-dot-dot line). (a) Fundamental phase-space projections; (b) simulton time evolutions of $v_1$; (c) simulton time evolutions of $v_2$ (note that solutions 1a and 3a overlap).

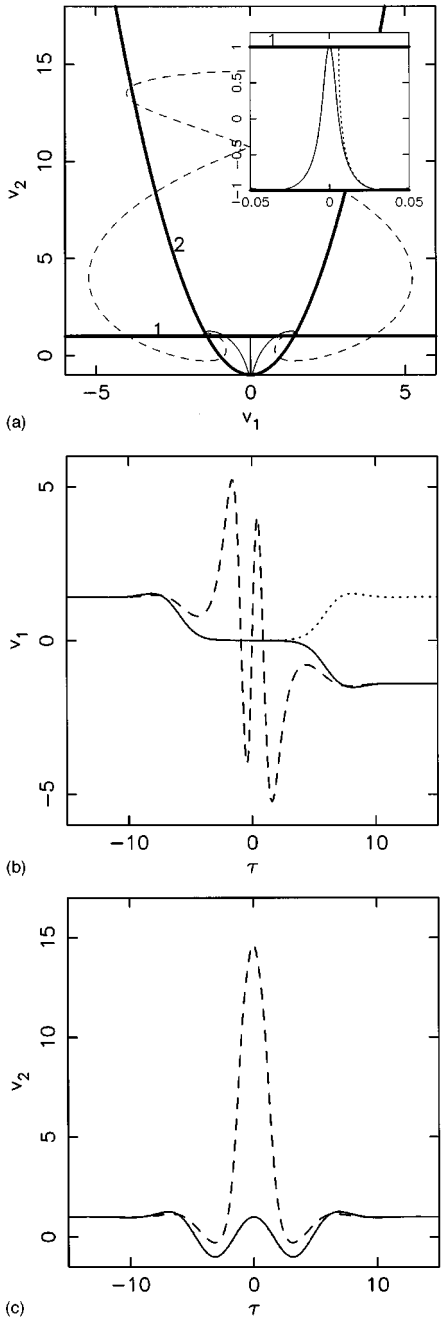


FIG. 9. Three simple higher-order simultons associated with $(\pm(2\rho)^{1/2},1)$ for case$(-,+)$ at $\rho=1$. Solution 1ah (solid line); solution 1bh (dashed line); solution 3ah (dotted line). (a) Fundamental phase-space projections (the inset is a close-up of phase projections near $v_1=0$); (b) simulton time evolutions of $v_1$; (c) simulton time evolutions of $v_2$ (note that solutions 1ah and 3ah overlap).

$$v_2=\frac{v_1^2}{\rho}-1, \tag{42a}$$

$$v_2=1. \tag{42b}$$

The boundary Eq. (42b) is marked with a ''1'' and the boundary Eq. (42a) is marked with a ''2'' in Fig. 7. For a classical particle, these boundaries act as potential barriers. A classical particle cannot go across these boundaries. However, a particle in this case has the interesting property that its mass is negative along one spatial direction. Meeting with these two boundaries, the particle will either return or go over with nonzero speed. Higher-order type-3 simultons can therefore occur.

Because of the novel feature of the particle, and the presence of these two boundaries, a rich family of simulton solutions exists. A particle that starts from one of these critical points can cross the two boundaries *or* return to the starting point *or* approach the other point. In short, any combination

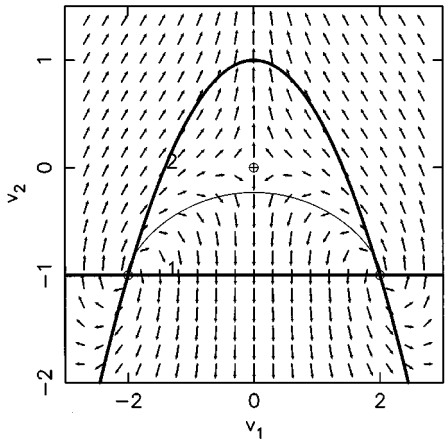


FIG. 10. Acceleration field for case$(-,-)$ at $\rho=2$ together with the boundary (heavy line) at $E=-\rho/2$ (the boundary $v_2=1-v_1^2/\rho$ is labeled with 2 and the boundary $v_2=-1$ is labeled with 1), and a fundamental type-1 solution (light line).

of these two boundaries with these two critical points would produce a simulton solution.

Some examples of the simplest fundamental and higher-order paths of both type 1 and type 3 at $\rho=1$ are shown in Fig. 8(a) and Fig. 9(a). Path 1b connects these two critical points directly. It represents the simplest type-1 solution for this case. Path 1bh is a higher-order type-1 path than path 1b. Path 1a is also a type-1 path but with the particle being reflected back from boundary 2. Note that the particle can be reflected between boundary 1 and 2 more than once, forming higher-order paths. Path 1ah is a higher-order path than path 1a. Path 3a is the simplest type-3 path connecting boundary 2. This path does not cross the axis $v_1=0$, so the resulting simulton only has one peak. Path 3ah is a higher-order type-3 path reflected by both boundaries 1 and 2. Path 3c is the simplest type-3 path connecting one of the critical points and boundary 1. Path 3b is the second simplest path similar to path 3a. There are more complicated higher-order simultons for each fundamental simulton. Here, we only show the simplest for the sake of simplicity.

### D. case$(-,-)$

The acceleration field is shown in Fig. 10. It has a saddle point at $(0,0)$ with one stable path and one unstable path leading to $(0,\pm\infty)$. There are no opposite accelerations pointing back to $(0,0)$ along the unstable path. Obviously, no simulton solutions are possible if a virtual particle starts from $(0,0)$. Point $(0,0)$ is always a saddle point, as eigenvalues around this point take different signs for any value of $\rho$.

Hence, only simultons associated with the other two unstable critical points at $(\pm\sqrt{2\rho},-1)$ can exist. Due to the nonzero values of these two points, these simultons will also appear with cw bright backgrounds. One of the necessary modulational stability conditions for simultons associated with $(\pm\sqrt{2\rho},-1)$ is $\rho\geqslant 2$ for this case [38,15]. This condition has been confirmed by Buryak and Kivshar's numerical simulations [15]. Under this condition, we find that eigenvalues are all complex for $\rho<8$. Hence the acceleration field appear with spiral accelerations around these two points. Their corresponding simultons therefore have oscillation tails. When $\rho>8$, these eigenvalues become real and positive. The spiral structures disappear. However, these two points are still unstable. Simulton solutions still exist except their tails no longer oscillate, as observed by Buryak and Kivshar [15].

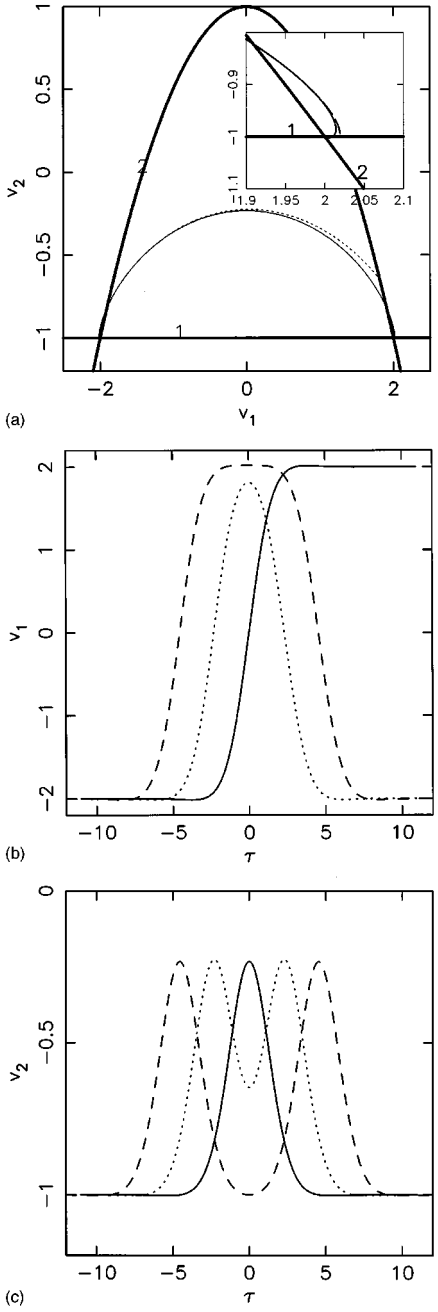


FIG. 11. Fundamental simultons of case$(-,-)$ at $\rho=2$, including (1) type-1 solution connecting both critical points (solid line), (2) type-3 solution connecting boundary 1 (dashed line), and (3) type-3 solution connecting boundary 2 (dotted line). (a) Phase-space projections (the inset is a close-up of phase-space projections near point $((2\rho)^{1/2},1)$; (b) simulton time evolutions of $v_1$; (c) simulton time evolutions of $v_2$.

The system again is not a normal Hamiltonian system as $s_1$ is negative. Therefore these two boundaries,

$$v_2=1-\frac{v_1^2}{\rho}, \tag{43a}$$

$$v_2=-1, \tag{43b}$$

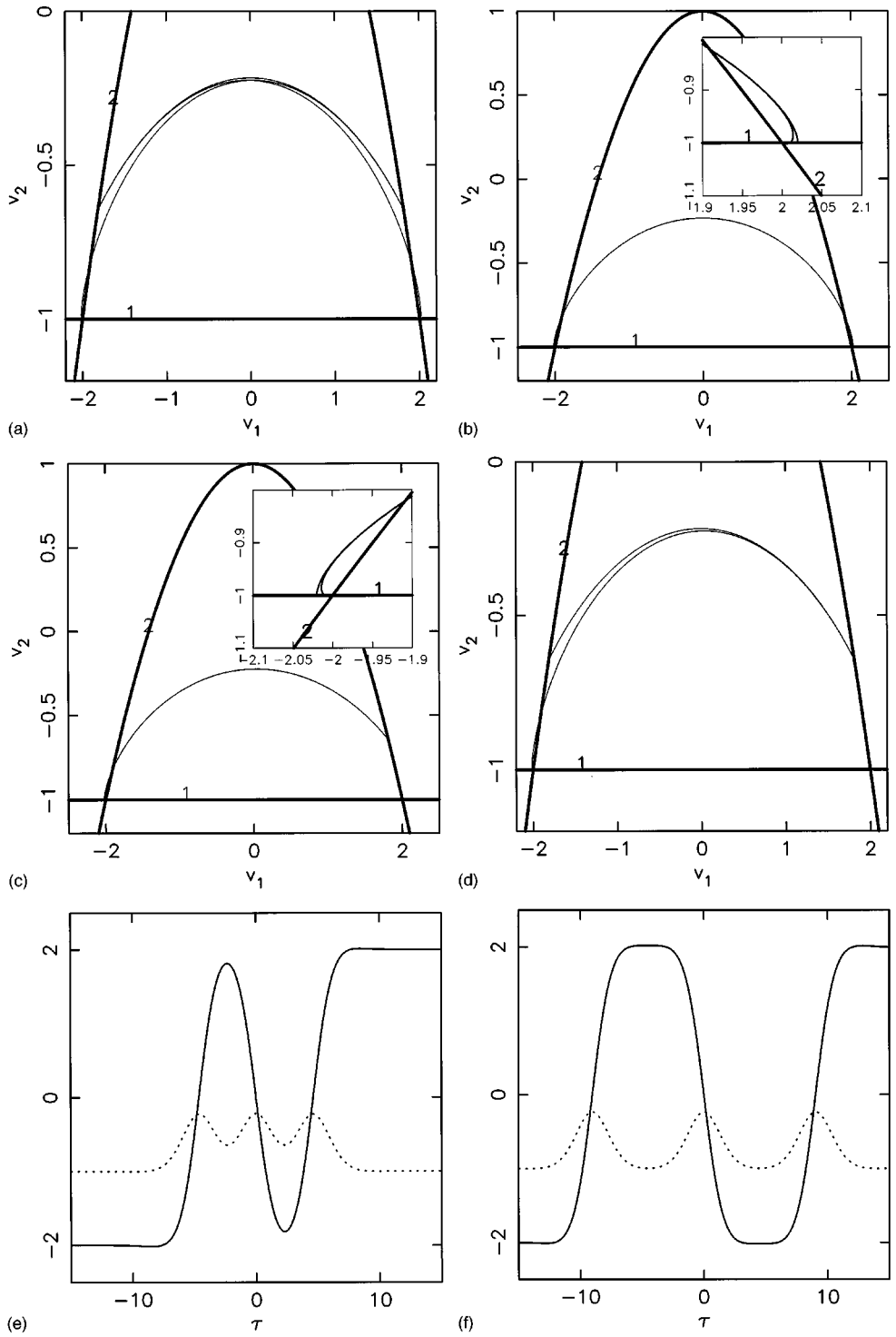


FIG. 12. Higher-order simultons of case$(-,-)$. (a) Phase-space projections of simulton (1), a type-1 solution reflected twice by boundary 2; (b) phase-space projections of simulton (2), a type-1 solution reflected twice by boundary 1 (the inset shows a close-up of phase-space projections near point $((2\rho)^{1/2},-1)$); (c) phase-space projections of simulton (3), a type-3 solution reflected by both boundary 1 and 2 (the inset shows a close-up of phase-space projections near point $(-(2\rho)^{1/2},-1)$); (d) phase-space projections of simulton (4), a type-3 solution reflected three times by boundary 2; (e) higher-order simulton time evolutions of simulton (1); (f) higher-order simulton time evolutions of simulton (2); (g) higher-order simulton time evolutions of simulton (3); (h) higher-order simulton time evolutions of simulton (4) ($v_1$, solid line; $v_2$, dotted line).

given by substituting $\dot{v}_1=\dot{v}_2=0$ into the Hamiltonian, can be crossed by a virtual particle. The boundary Eq. (43b) is marked with a ''1'' and the boundary Eq. (43a) is marked with a ''2'' in Fig. 10.

### *1. Fundamental simultons*

Similarly to the previous case, a particle that starts from one of these two points will take a spiral path with the same

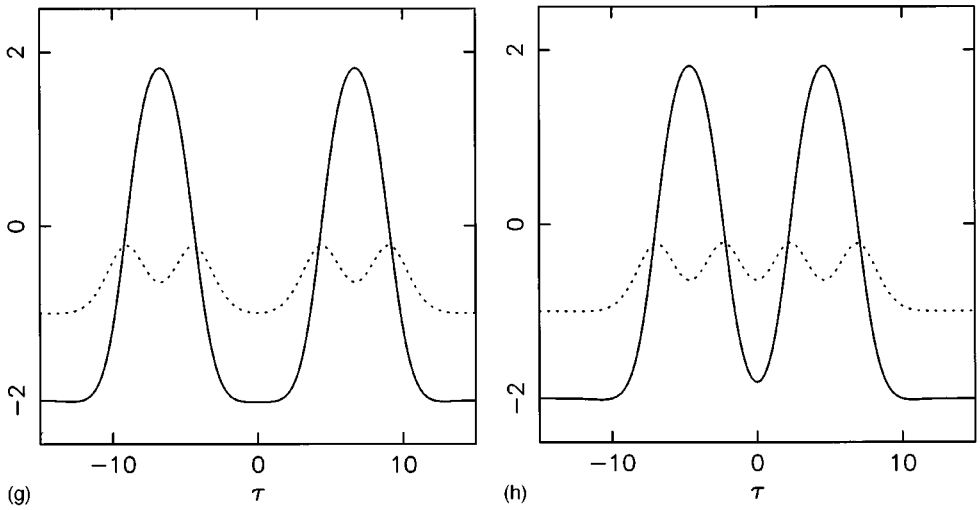


FIG. 12 (*Continued*).

helicity as the acceleration field around the point if $\rho<8$. Without losing generality, we may analyze a particle that starts from point $(-\sqrt{2\rho},-1)$. After leaving this point, the particle can go upward and cross the boundary given by Eq. (43a), or go downward and cross the boundary given by Eq. (43b). However, there are no opposite accelerations along these two boundaries when $v_1<0$. Type-3 paths hence are impossible within the area $v_1<0$. Since there are an infinite number of unstable paths connected to point $(-\sqrt{2\rho},-1)$, we can always find paths leading to the area $v_1>0$. Once a particle crosses over $v_1=0$, it then can form two different type-3 paths, (1) associated with the boundary 2, Eq. (43a), and (2) associated with boundary 1, Eq. (43b). The particle can also approach the other point $(\sqrt{2\rho},-1)$, forming a type-1 path. Numerical solutions are shown in Fig. 11. These simultons were known known previously [15]. These three types of simulton form a family of fundamental solutions.

#### *2. Higher-order simultons*

Similarly to the previous case, combinations among these boundaries and critical points result in higher order type-1 and type-3 simultons. Some simple higher-order simultons are the following.

(1) Simulton (1), shown in Fig. 12(a), is a type-1 path connecting the two critical points and the boundary 2, Eq. (43a).

(2) Simulton (2), shown in Fig. 12(b), is a type-1 path connecting the two critical points with the boundary 1, Eq. (43b).

(3) Simulton (3), shown in Fig. 12(c), is a type-3 path connecting one of the two critical points with both the boundaries 1 and 2.

(4) Simulton (4), shown in Fig. 12(d), is a type-3 path connecting one of the two critical points with the boundary 2 only. Obviously, a similar type-3 path connecting one of the two critical points with the boundary 1 only also exists.

The corresponding simulton time-evolutions are shown in Figs. 12(e)–12(h).

## IV. SIMULTON SOLUTIONS TO SPATIAL EQUATIONS

### A. One-dimensional simultons

The spatial equations have the same forms as temporal equations. They can be written as [9,13]:

$$i\frac{\partial v_1}{\partial \xi}+\frac{\partial^2 v_1}{\partial r^2}+v_1^* v_2-v_1=0, \tag{44a}$$

$$i\sigma\frac{\partial v_2}{\partial \xi}+\frac{\partial^2 v_2}{\partial r^2}+\tfrac{1}{2}v_1^2-\rho v_2=0, \tag{44b}$$

where $\sigma=k_2/k_1$, $\rho=(2\beta+\delta k)\sigma/\beta$, and $\xi=\beta z$. Here, $k_1$ and $k_2$ are wave numbers along the $z$ direction, $\delta k$ is the wave-vector mismatch, and $\beta$ is a measure of the effective linear phase mismatch between both waves. In realistic cases $\sigma\approx 2$ [17].

As $\rho>0$, the solutions to spatial equations simply are solutions of case$(+,+)$.

### B. Spatial simultons in higher dimensions

Based on previous publications [17,40,23], the basic equations written in $n+1$ dimensions, $n=2,3$, can be written as:

$$i\frac{\partial v_1}{\partial z}+\nabla^2 v_1-v_1+v_1^* v_2=0, \tag{45a}$$

$$i\sigma\frac{\partial v_2}{\partial z}+\nabla^2 v_2-\rho v_2+\tfrac{1}{2}v_1^2=0, \tag{45b}$$

where $\rho$ and $\sigma$ have the same definition as for the one-dimensional equations.

One seeks radially symmetric solutions to the above equations. Substituting the ansatz

$$v_i=v_i(r), \quad i=1,2, \tag{46}$$

into the above equations gives

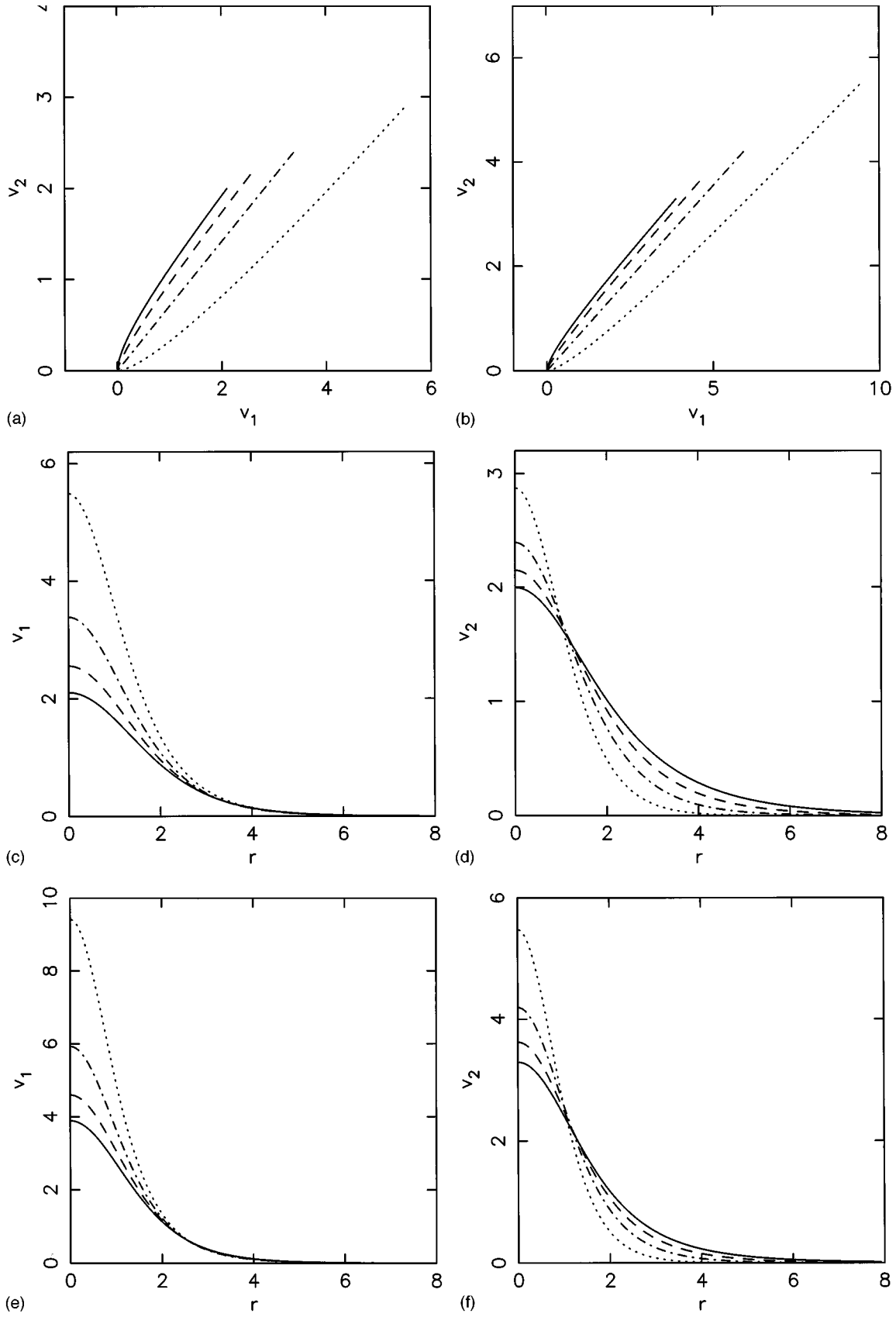


FIG. 13. Higher-dimensional spatial simultons where $\rho = 0.3$ (solid line), 0.5 (dashed line), 1.0 (dash-dotted line), and 3.0 (dotted line). (a) Phase-space projections for (2+1)-dimensional spatial simultons; (b) phase-space projections for (3+1)-dimensional spatial simultons; (c) fundamental (2+1)-dimensional spatial simulton radial dependence of $v_1$; (d) fundamental (2+1)-dimensional spatial simulton radial dependence of $v_2$; (e) fundamental (3+1)-dimensional spatial simulton radial dependence of $v_1$; (f) fundamental (3+1)-dimensional spatial simulton radial dependence of $v_2$.

$$i\frac{\partial v_1}{\partial z}+\frac{\partial^2 v_1}{\partial r^2}+\frac{(n-1)}{r}\frac{dv_1}{dr}-v_1+v_1^* v_2=0, \quad (47a)$$

$$i\sigma\frac{\partial v_2}{\partial z}+\frac{\partial^2 v_2}{\partial r^2}+\frac{(n-1)}{r}\frac{dv_2}{dr}-\rho v_2+\tfrac{1}{2}v_1^2=0. \quad (47b)$$

Compared with the equations of case$(+,+)$, the above equations take the same forms except with two extra ''frictional terms'' [41], $[(n-1)/r](dv_m/dr)$. Obviously, spatial simulton solutions must satisfy the following boundary conditions:

$$\frac{dv_i}{dr}=0 \quad \text{at } r=0, \quad i=1,2. \quad (48)$$

This condition is necessary so that these two ''frictional terms'' do not become singular at $r=0$. Following the arguments for the existing of simulton solutions of case$(+,+)$, one can easily prove that there exists a family of simulton solutions for arbitrary values of $\rho$. These solutions were found recently by many people [23,17,42] and were observed by Torruellas *et al.* [43] experimentally. Compared with the simultons of case$(+,+)$, these spatial simultons usually have higher amplitudes in order to compensate for the energy loss of the virtual particle due to the presence of ''friction.'' The path also becomes a straight line at $\rho=1$. Approximate solutions were found by Hayata and Koshiba [40] for $n$-dimensional wave equations, although the case of $n>3$ appears to be inapplicable to optical systems. The corresponding exact numerical result for fundamental simultons is given below. Paths for different values of $\rho$ are shown in Fig. 13(a) and Fig. 13(b). These paths also bend slightly upward for $\rho<0$ and bend slightly downward for $\rho>0$. The topological structure in this case is nearly identical to that in the one-dimensional case$(+,+)$, previously discussed. We therefore conclude that there also exists a new family of higher-order spatial simultons corresponding to the odd-number-peak simultons previously studied in case$(+,+)$. Due to the boundary condition Eq. (48), the even-number-peak simultons in case$(+,+)$ have no correspondence in the spatial case. Paths of these higher-order spatial simultons are shown in Fig. 14(a). Their profiles are shown in Fig. 14(b) and Fig. 14(c). The numerical method involved in finding these spatial simultons is a combination of the standard shooting method and a routine of searching for the correct initial energy. These solutions can be thought of as behaving like classical ''excited states'' or ''resonances,'' although they are probably not stable.

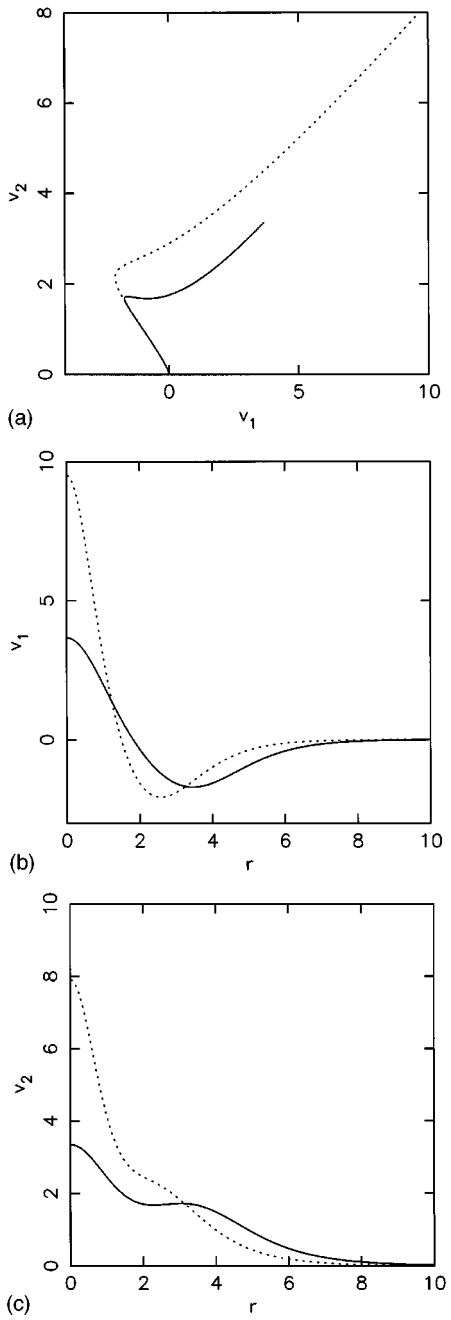


FIG. 14. Higher-order $(2+1)$-dimensional (solid line) and $(3+1)$-dimensional spatial (dotted line) simultons at $\rho=0.5$. (a) Phase-space projection; (b) $v_1$; (c) $v_2$.

## V. CONCLUSIONS

The basic equations which describe the $\chi^{(2)}$ cascaded nonlinearity in the presence of dispersion or diffraction have remained unsolved for almost 20 years. Previous methods of obtaining solitary solutions were unable to to find all possible solutions. In this paper, instead of using complex mathematical analysis, we have used simple topological arguments combined with numerical integration to prove the existence of simulton solutions. Compared with traditional methods, such as inverse scattering or inserting an ansatz, this method has been proved to be a much more efficient technique of finding solutions. This method may also be applied to other, similar, vector systems.

We have confirmed that the system is a one-parameter system by transforming the basic equation into eight sets of one-parameter equations. The number of possible cases has then been reduced to four based on topological arguments. General numerical solutions are then found by studying the corresponding acceleration fields, and integrating the relevant equations

In case$(+,+)$, general solutions for arbitrary values of $\rho$ have been found. The previous known analytical solution for this case is a special case with $\rho=1$ (known as the phase-matching condition) of the general solutions. This is encouraging for experiments, as the strict phase-matching condition no longer necessarily has to be satisfied and only low power

is required. These solutions were also found numerically by Buryak and Kivshar [11,18] and Torner *et al.* [13,12], thus verifying our numerical algorithm. It is interesting to note that higher-order simultons with multiple peaks exist when $\rho<1$.

Simultons exist only for discrete values of $\rho$ in case $(+,-)$. One analytical simulton known previously corresponds to a special case, $\rho=1$. The whole family of simultons in this case is known to be unstable due to the modulational instability resulting from their cw backgrounds [38].

The case$(-,+)$ has a rich family of simulton solutions because of the novel features provided by the system. The virtual particle with negative mass along one spatial direction can cross a potential boundary. This behavior is different from that of a classical particle with positive mass independent of spatial direction. It hence introduces complexity but also interesting features to the system. All solutions are generally classified into two categories according to the critical point with which they associate. Simultons associated with point $(0,0)$ are found only for discrete values of $\rho$. We again find that a previous known analytical simulton corresponds to a special case at $\rho=2$. Associated with the other two spiral critical points, general topological and nontopological simultons with many varieties exist for continuous values of $0<\rho\leqslant 2$. Higher-order simultons also exist for each type of simulton. Numerical investigation of the stabilities of these simultons is currently being carried out. All general solutions of this case were unknown before.

For case$(-,-)$, both topological and nontopological simultons exist for arbitrary values of $\rho>2$ because of the modulational stability condition. Similarly to the previous case, higher-order simultons exist for each type of simulton. Solutions of this case were known previously [15,16].

Finally, we briefly discuss spatial equations with the topological method that we have developed. General spatial simultons for higher-dimensional systems exist. The fundamental solutions in two dimensions have been experimentally observed already [43]. We also find an additional family of higher-order spatial simultons.

In conclusion, these simulton solutions have revealed some interesting properties of this dynamical system described by coupled nonlinear partial differential equations. While the simultons themselves may have potential applications in communications and optical logic gates, they also pose fundamental challenges for the better understanding of vector nonlinear wave equations.


[1] Y. N. Karamzin and A. P. Sukhorukov, Sov. Phys. JETP **41**, 414 (1976).
[2] Y. N. Karamzin, A. P. Sukhorukov, and T. S. Filipchuk, Moscow Univ. Phys. Bull. **19**, 91 (1978).
[3] G. Valiulis and K. Staliunas, Lithuanian Phys. J. **31**, 38 (1991).
[4] M. J. Werner and P. D. Drummond, Quantum Electron. Laser Sci. Tech. Dig. Ser. **12**, 290 (1993).
[5] M. J. Werner and P. Drummond, J. Opt. Soc. Am. B **10**, 2390 (1993).
[6] R. Schiek, J. Opt. Soc. Am. B **10**, 1848 (1993).
[7] M. J. Werner and P. D. Drummond, Opt. Lett. **19**, 613 (1994).
[8] M. A. Karpierz and M. Sypek, Opt. Commun. **110**, 75 (1994).
[9] C. R. Menyuk, R. Schiek, and L. Torner, J. Opt. Soc. Am. B **11**, 2434 (1994).
[10] K. Hayata and M. Koshiba, Phys. Rev. A **50**, 675 (1994).
[11] A. V. Buryak and Y. S. Kivshar, Opt. Lett. **19**, 1612 (1994).
[12] L. Torner, C. R. Menyuk, and G. I. Stegeman, J. Opt. Soc. Am. B **12**, 889 (1995).
[13] L. Torner, Opt. Commun. **114**, 136 (1995).
[14] L. Torner, C. R. Menyuk, and G. I. Stegeman, Opt. Lett. **19**, 1615 (1994).
[15] A. V. Buryak and Y. S. Kivshar, Phys. Rev. A **51**, R41 (1995).
[16] A. V. Buryak and Y. S. Kivshar, Opt. Lett. **20**, 834 (1995).
[17] A. V. Buryak, Y. S. Kivshar, and V. V. Steblina, Phys. Rev. A **52**, 1670 (1995).
[18] A. V. Buryak and Y. S. Kivshar, Phys. Lett. A **197**, 407 (1995).
[19] M. Hénon and C. Heiles, Astron. J. **69**, 73 (1964).
[20] R. DeSalvo *et al.*, Opt. Lett. **17**, 28 (1992).
[21] R. Danielius *et al.*, Opt. Lett. **18**, 574 (1993).
[22] S. Nitti, H. M. Tan, G. P. Banfi, and V. Degiorgio, Opt. Commun. **106**, 263 (1994).
[23] L. Torner, C. R. Menyuk, W. E. Torruellas, and G. I. Stegeman, Opt. Lett. **20**, 13 (1995).
[24] L. Torner *et al.*, Opt. Commun. **121**, 149 (1995).
[25] M. J. Konopnicki, P. D. Drummond, and J. H. Eberly, Opt. Commun. **36**, 313 (1981).
[26] M. J. Konopnicki and J. H. Eberly, Phys. Rev. A **49**, 2567 (1981).
[27] J. H. Eberly, Opt. Commun. **36**, 313 (1981).
[28] P. D. Drummond, Opt. Commun. **49**, 219 (1984).
[29] R. Grobe, F. T. Hioe, and J. J. Eberly, Phys. Rev. Lett. **73**, 3183 (1994).
[30] J. H. Eberly, M. L. Pons, and H. R. Haq, Phys. Rev. Lett. **72**, 56 (1994).
[31] P. D. Drummond and S. J. Carter, J. Opt. Soc. Am. B **4**, 1565 (1987).
[32] L. F. Mollenauer, R. H. Stolen, and J. P. Gordon, Phys. Rev. Lett. **45**, 1905 (1980).
[33] S. Coleman, *Aspects of Symmetry* (Cambridge University Press, Cambridge, England, 1989).
[34] N. H. Christ and T. D. Lee, Phys. Rev. D **12**, 1606 (1975).
[35] R. Friedberg and T. D. Lee, Phys. Rev. D **15**, 1694 (1977).
[36] T. D. Lee, in *Particle Physics and Introduction to Field Theory*, revised and updated first edition, edited by H. Feshbach *et al.* (Harwood Academic, Chur, Switzerland, 1988), Vol. 1.
[37] G. D. Boyd *et al.*, Appl. Phys. Lett. **5**, 234 (1964).
[38] H. He, P. D. Drummond, and B. A. Malomed, Opt. Commun. **123**, 395 (1996).
[39] S. Trillo and P. Ferro, Opt. Lett. **20**, 438 (1995).
[40] K. Hayata and M. Koshiba, Phys. Rev. Lett. **71**, 3275 (1993).
[41] R. Friedberg, T. D. Lee, and A. Sirlin, Phys. Rev. D **13**, 2739 (1976).
[42] V. V. Steblina, Y. S. Kivshar, M. Lisak, and B. A. Malomed, Opt. Commun. **118**, 345 (1995).
[43] W. E. Torruellas *et al.*, Phys. Rev. Lett. **74**, 5036 (1995).